Inorg. Chem. **2007**, *46*, 3623–3631

Boron and Aluminum Complexes of Sterically Demanding Phosphinimines and Phosphinimides

Silke Courtenay, Denise Walsh, Sarah Hawkeswood, Pingrong Wei, Anjan Kumar Das, and Douglas W. Stephan*

Department of Chemistry & Biochemistry, University of Windsor, Windsor, Ontario, Canada N9B 3P4

Received January 9, 2007

Reactions of sterically demanding phosphinimines R_3PNH [R = *i*-Pr (**1**), *t*-Bu (**2**)] were examined. Reactions with $B(C_6F_5)_3$ formed the adducts $(R_3PNH)B(C_6F_5)_3$ [R = *i*-Pr (**3**), *t*-Bu (**4**)] in high yield. On the other hand, **2** reacts with $HB(OBu)_2$, evolving H_2 to give *t*-$Bu_3PNB(OBu)_2$ (**5**). The reaction of 2 equiv of **2** with $BH_3{\cdot}SMe_2$ affords the species $(t\text{-}Bu_3PN)_2BH$ (**6**). In contrast, the reaction of *n*-Bu(*t*-Bu)$_2$PNH with $BH_3{\cdot}SMe_2$ results in the formation of the robust adduct *n*-Bu(*t*-Bu)$_2$PNH·BH_3 (**8**). An alternative route to borane–phosphinimide complexes involves Me_3SiCl elimination, as exemplified by the reaction of BCl_2Ph with *n*-$Bu_3PNSiMe_3$, which gives the product *n*-$Bu_3PNBCl(Ph)$ (**9**). The corresponding reactions of the parent phosphinimines **1** and **2** with $AlH_3{\cdot}NMe_2Et$ give the dimers $[(\mu\text{-}i\text{-}Pr_3PN)AlH_2]_2$ (**10**) and $[(\mu\text{-}t\text{-}Bu_3PN)AlH_2]_2$ (**11**). Species **11** reacts further with $Me_3SiO_3SCF_3$ to provide $[(\mu\text{-}t\text{-}Bu_3PN)AlH(OSO_2CF_3)]_2$ (**12**). The reaction of the lithium salt $[t\text{-}Bu_3PNLi]_4$ (**13**) with BCl_3 proceeds smoothly to give *t*-Bu_3PNBCl_2 (**14**), which is readily alkylated to give *t*-Bu_3PNBMe_2 (**15**). Subsequent reaction of **15** with $B(C_6F_5)_3$ results in methyl abstraction and the formation of $[(\mu\text{-}t\text{-}Bu_3PN)BMe]_2[MeB(C_6F_5)_3]_2$ (**16**). The reaction of **13** in a 2:1 ratio with BCl_3 gives the salt $[(t\text{-}Bu_3PN)_2B]Cl$ (**17**). This species can be methylated to give $(t\text{-}Bu_3PN)_2BMe$ (**18**), which undergoes subsequent reaction with $[Ph_3C][X]$ (X = $[B(C_6F_5)_4]$, $[PF_6]$) to form the related salts $[(t\text{-}Bu_3PN)_2B][B(C_6F_5)_4]$ (**19**) and $[(t\text{-}Bu_3PN)_2B][PF_6]$ (**20**), respectively. Analogous reactions with $[Ph_3C][BF_4]$ afforded $[t\text{-}Bu_3PNBF_2]_2$ (**21**). Compounds **3**, **4**, **6**, **8**, **11**, **12**, **17**, **19**, and **21** were characterized by X-ray crystallography.

Introduction

Transition-metal complexes incorporating phosphinimide ligand complexes have proven to be an active area of research in recent years. While Cavell and co-workers have made a number of reports on the extremely interesting carbenoid complexes for a variety of metals derived from the phosphinimines of 1,1-diphosphinomethanes,[1−4] we have probed the chemistry of a variety of metal phosphinimide complexes, ultimately developing commercially viable early-transition-metal catalysts for olefin polymerization based on titanium phosphinimides. This latter work has been recently reviewed.[5] In contrast, the related chemistry of main-group phosphinimines and phosphinimides has recently drawn much less attention. Dehnicke and Weller described much of the older literature in a review nearly 10 years ago.[6] More recently, we and others have begun to examine main-group phosphinimine and phosphinimide derivatives. For example, in some elegant work, Meyer and co-workers[7,8] have demonstrated that phosphinimines themselves undergo metathesis with imines and catalyze imine/imine and imine/carbodiimine cross-metathesis. We have probed the synthesis, structure, and reactivity of lithium,[9] magnesium,[10,11] silicon, tin, and germanium[12] as well as aluminum alkyl[13] phosphin-

* To whom correspondence should be addressed. E-mail: stephan@uwindsor.ca. Fax: 519-973-7098.

(1) Aparna, K.; Babu, R. P. K.; McDonald, R.; Cavell, R. G. *Angew. Chem., Int. Ed.* **2001**, *40*, 4400.
(2) Babu, R. P. K.; McDonald, R.; Cavell, R. G. *Chem. Commun.* **2000**, *6*, 481.
(3) Kasani, A.; Babu, R. P. K.; McDonald, R.; Cavell, R. G. *Angew. Chem., Int. Ed.* **1999**, *38*, 1483.
(4) Kasani, A.; McDonald, R.; Cavell, R. G. *Chem. Commun.* **1999**, 1993.
(5) Stephan, D. W. *Organometallics* **2005**, *24*, 2548.
(6) Dehnicke, K.; Weller, F. *Coord. Chem. Rev.* **1997**, *158*, 103.
(7) Bell, S. A.; Meyer, T. Y.; Geib, S. J. *J. Am. Chem. Soc.* **2002**, *124*, 10698.
(8) Burland, M. C.; Meyer, T. Y. *Inorg. Chem.* **2003**, *42*, 3438.
(9) Courtenay, S.; Wei, P.; Stephan, D. W. *Can. J. Chem.* **2003**, *81*, 1471.
(10) Wei, P.; Stephan, D. W. *Organometallics* **2003**, *22*, 601.
(11) Hollink, E.; Wei, P.; Stephan, D. W. *Can. J. Chem.* **2005**, *83*, 430.
(12) Courtenay, S.; Ong, C. M.; Stephan, D. W. *Organometallics* **2003**, *22*, 818.

10.1021/ic0700351 CCC: $37.00
Published on Web 03/23/2007

Chart 1

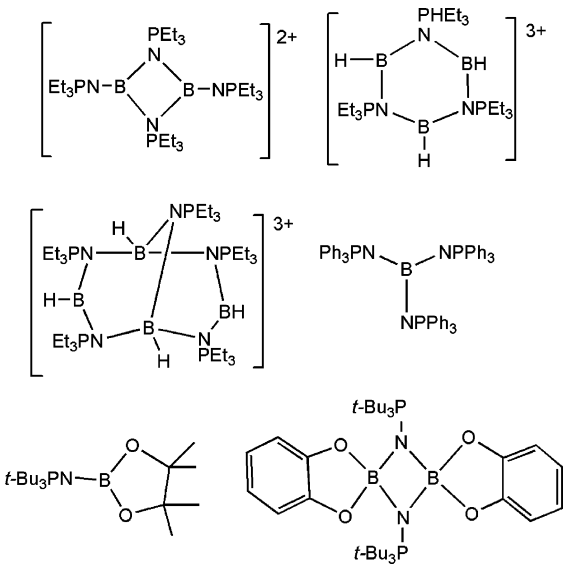

imide derivatives. Our interest in the group 3 phosphinimine and phosphinimide chemistry has prompted continuing investigations. Boron phosphinimide derivatives of sterically less demanding phosphinimides including such compounds as $[(Et_3PN)_2B)_2]^{2+}$,[14] $[(Et_3PNBH)_3]^{3+}$,[15] $[(Et_3PNBH)_4NPEt_3]^{3+}$,[16] or $[(Ph_3PN)_3B]$[17] have been described by Dehnicke and Weller. Known aluminum phosphinimides exhibit dimeric structures exclusively.[6,13] Recently, we probed steric effects that control the reactions of catechol and pinachol boranes with phosphinimines.[18,19] In these cases, both monomeric and dimeric complexes, such as $R_3PNB(O_2C_2Me_4)$ and $[R_3PNB(O_2C_6H_4)]_2$, were prepared as a result of the incorporation of sterically demanding phosphinimide ligands (Chart 1). We have also previously communicated a case where such large steric demands prompt the spontaneous formation of the salt $[(t\text{-}Bu_3PN)_2B]Cl$.[20] In this present full report, we include this latter chemistry and related work, exploring several synthetic pathways to both boron and aluminum complexes with sterically demanding phosphinimine and phosphinimide ligands. The range of products is described, and in selected cases, the chemistry of the resulting species is also probed.

Experimental Section

General Data. All preparations were performed under an atmosphere of dry O_2-free N_2 employing either Schlenk-line techniques or a Vacuum Atmospheres inert-atmosphere glovebox. Solvents were purified by employing Grubbs-type column systems manufactured by Innovative Technologies or were distilled from the appropriate drying agents under N_2. ^1H and $^{13}C\{^1H\}$ NMR spectra were recorded on Bruker Avance 300 and 500 spectrometers operating at 300 and 500 MHz, respectively. Deuterated benzene, toluene, and methylene chloride were purchased from Cambridge Isotopes Laboratories, freeze−pump−thaw−degassed (three times), and vacuum distilled from the appropriate drying agents. Trace amounts of protonated solvents were used as references, and ^1H and $^{13}C\{^1H\}$ NMR chemical shifts are reported relative to $SiMe_4$. $^{31}P\{^1H\}$, $^{11}B\{^1H\}$, $^{27}Al\{^1H\}$, and ^{19}F NMR spectra were referenced to external 85% H_3PO_4, $BF_3{\cdot}Et_2O$, $AlCl_3$ in H_2O, and $CFCl_3$, respectively. Combustion analyses were performed at the University of Windsor Chemical Laboratories employing a Perkin-Elmer CHN analyzer. R_3PNH [R = *i*-Pr (**1**), *t*-Bu (**2**)][21] and $[t\text{-}Bu_3PNLi]_4$[9] (**13**) were prepared by published methods. *n*-Bu(*t*-Bu)$_2$PNH (**7**) was prepared via the method previously described, with the appropriate replacement of the precursor phosphine.[21]

Synthesis of $(R_3PNH)B(C_6F_5)_3$ [R = *i*-Pr (3), *t*-Bu (4)]. These complexes were prepared in a similar manner, and thus only a single representative preparation is described. To a solution of **2** (250 mg, 1.150 mmol) in 5 mL of CH_2Cl_2 was added $B(C_6F_5)_3$ (589 mg, 1.150 mmol). The solution was stirred for 1 h and concentrated, resulting in the formation of colorless crystals of **4** in 95% yield. **3**. Yield: 93%. ^1H NMR (CD_2Cl_2): 2.97 (s, br, 1H), 2.17 (m, 3H), 1.20 (dd, $^3J_{P-H}$ = 16 Hz, $^3J_{H-H}$ = 7 Hz, 18H). $^{13}C\{^1H\}$ NMR (CD_2Cl_2): 147.0−135.8 (br m), 25.7 (d, $^1J_{P-C}$ = 55 Hz), 17.5 (s). $^{31}P\{^1H\}$ NMR (CD_2Cl_2): 64.0. $^{11}B\{^1H\}$ NMR (CD_2Cl_2): −7.5 (s). ^{19}F NMR (CD_2Cl_2): −55.4 (d, $^3J_{F-F}$ = 20 Hz, 6F), −83.0 (t, $^3J_{F-F}$ = 20 Hz, 3F), −87.8 (m, 6F). Anal. Calcd for $C_{27}H_{22}BF_{15}NP$: C, 45.34; H, 3.10; N, 1.96. Found: C, 44.98; H, 3.18; N, 1.88. **4**. ^1H NMR (CD_2Cl_2): 3.30 (s, br, 1H), 1.41 (d, $^3J_{P-H}$ = 14 Hz, 27 H). $^{13}C\{^1H\}$ NMR (CD_2Cl_2): 149.9−135.6 (br m), 41.0 (d, $^1J_{P-C}$ = 42 Hz), 29.4 (s). $^{31}P\{^1H\}$ NMR (CD_2Cl_2): 78.8. $^{11}B\{^1H\}$ NMR (CD_2Cl_2): −9.5 (s). ^{19}F NMR (CD_2Cl_2): −51.4 (d, $^3J_{F-F}$ = 11 Hz, 6F), −82.8 (t, $^3J_{F-F}$ = 21 Hz, 3F), −87.9 (m, 6F). Anal. Calcd for $C_{30}H_{28}BF_{15}NP$: C, 49.41; H, 3.87; N, 1.92. Found: C, 49.16; H, 4.08; N, 2.07.

Synthesis of $t\text{-}Bu_3PNB(OBu)_2$ (5). To a solution of **2** (30 mg, 0.138 mmol) in 5 mL toluene was added a solution of $HB(OBu)_2$ (46 μL, 3 M in THF, 0.138 mmol). The solution was stirred overnight, and the solvent was evaporated, leaving the product as a fine white powder in 95% yield. ^1H NMR (C_6D_6): 4.17 (t, $^3J_{H-H}$ = 6 Hz, 4H), 1.90 (m, 4H), 1.57 (m, 4H) 1.30 (d, $^3J_{P-H}$ = 13 Hz, 27H), 0.97 (t, $^3J_{H-H}$ = 7 Hz, 6H). $^{13}C\{^1H\}$ NMR (C_6D_6): 63.6 (s), 40.6 (d, $^1J_{P-C}$ = 52 Hz), 35.4 (s), 30.0 (s), 20.3 (s), 14.7 (s). $^{31}P\{^1H\}$ NMR (C_6D_6): 38.4. $^{11}B\{^1H\}$ NMR (C_6D_6): 17.1. Anal. Calcd for $C_{20}H_{45}BNO_2P$: C, 64.34; H, 12.15; N, 3.75. Found: C, 64.20; H, 12.02; N, 3.71.

Synthesis of $(t\text{-}Bu_3PN)_2BH$ (6). To a solution of **2** (150 mg, 0.690 mmol) in toluene (10 mL) was added $BH_3{\cdot}SMe_2$ (173 μL, 2 M in diethyl ether). The resulting suspension was refluxed for 1 h and cooled to 25 °C, and the solvent was removed in vacuo. The product was isolated as a white powder in 75% yield. Uptake of the powder in a minimum amount of toluene and addition of a couple of drops of hexane resulted in isolation of X-ray-quality crystals. ^1H NMR (C_6D_6) partial: 1.37 (d, $^3J_{P-H}$ =12 Hz, 54H). $^{13}C\{^1H\}$ NMR (C_6D_6): 40.8 (d, $^1J_{P-C}$ = 50 Hz), 30.5 (s). $^{31}P\{^1H\}$ NMR (C_6D_6): 31.2. $^{31}P\{^1H\}$ NMR (CD_2Cl_2): 35.4. $^{11}B\{^1H\}$ NMR

(13) Ong, C. M.; McKarns, P.; Stephan, D. W. *Organometallics* **1999**, *18*, 4197.
(14) Moehlen, M.; Neumuller, B.; Faza, N.; Muller, C.; Massa, W.; Dehnicke, K. *Z. Anorg. Allg. Chem.* **1997**, *623*, 1567.
(15) Möhlen, M.; Neumüller, B.; Harms, K.; Krautscheid, H.; Fenske, D.; Diedenhofen, M.; Frenking, G.; Dehnicke, K. *Z. Anorg. Allg. Chem.* **1998**, *624*, 1105.
(16) Möhlen, M.; Neumüller, B.; Dehnicke, K. *Z. Anorg. Allg. Chem.* **1999**, *625*, 197.
(17) Moehlen, M.; Neumueller, B.; Dehnicke, K. *Z. Anorg. Allg. Chem.* **1998**, *624*, 177.
(18) Hawkeswood, S.; Stephan, D. W. *Dalton Trans.* **2005**, 2182.
(19) Hawkeswood, S.; Wei, P.; Gauld, J. W.; Stephan, D. W. *Inorg. Chem.* **2005**, *44*, 4301.
(20) Courtenay, S.; Mutus, J. Y.; Schurko, R. W.; Stephan, D. W. *Angew. Chem., Int. Ed.* **2002**, *41*, 498−501.
(21) Stephan, D. W.; Stewart, J. C.; Guerin, F.; Courtenay, S.; Kickham, J.; Hollink, E.; Beddie, C.; Hoskin, A.; Graham, T.; Wei, P.; Spence, R. E. v. H.; Xu, W.; Koch, L.; Gao, X.; Harrison, D. G. *Organometallics* **2003**, *22*, 1937.

(C_6D_6): 24.6 (br). Anal. Calcd for $C_{24}H_{55}BN_2P_2$: C, 64.86; H, 12.47; N, 6.30. Found: C, 64.20; H, 12.82; N, 5.96.

Synthesis of *n*-Bu(*t*-Bu)$_2$PNH·BH$_3$ (8). To a solution of phosphinimine **7** (0.150 g, 0.690 mmol) in 10 mL of hexane was added BH_3·SMe_2 (2 M, 0.173 mL, 0.345 mmol) in diethyl ether. The solution was stirred for 4 h and filtered. X-ray-quality crystals were collected from the hexane supernatant kept at −30 °C. Yield: 87%. ^{1}H NMR (C_6D_6): 1.76 (m, 2H), 1.60 (m, 2H), 0.1.26 (sextet, 2H, $^3J_{H-H}$ = 7 Hz), 0.89 (d, 18H, $^3J_{P-H}$ = 14 Hz), 0.84 (t, 3H, $^3J_{H-H}$ = 8 Hz). ^{31}P{^{1}H} NMR (C_6D_6): 61.6. ^{13}C{^{1}H} NMR (C_6D_6): 27.7, 25.8 (d, $^3J_{P-C}$ = 19 Hz), 25.5 (d, $^2J_{P-C}$ = 26 Hz), 19.0 (d, $^1J_{P-C}$ = 30 Hz), 14.1. ^{11}B{^{1}H} NMR (C_6D_6): −21.0. Anal. Calcd: C, 62.35; H, 13.52; N, 6.06. Found: C, 62.02; H, 13.22; N, 5.90.

Synthesis of *n*-Bu$_3$PNBCl(Ph) (9). A solution of BCl_2Ph (0.2 mL, 1.542 mmol) in 5 mL of toluene was slowly added via syringe to a solution of *n*-$Bu_3PNSiMe_3$ (0.446 g, 1.541 mmol) in 35 mL of toluene. The Schlenk flask was put under a static vacuum and stirred for 72 h. The solvent was removed in vacuo, and the remaining white solid was washed with *n*-pentane. ^{1}H NMR (C_6D_6): 8.72 (d, 2H, $^3J_{H-H}$ = 7 Hz), 7.47 (t, 2H, $^3J_{H-H}$ = 7 Hz), 7.28 (t, $^3J_{H-H}$ = 7 Hz), 1.60 (m, 6H), 1.22 (m, 6H), 1.02 (tq, 6H, $^3J_{H-H}$ = 7 Hz, $^3J_{H-H}$ = 7 Hz), 0.73 (t, 9H, $^3J_{H-H}$ = 7 Hz). ^{31}P{^{1}H} NMR (C_6D_6): 39.8. ^{13}C{^{1}H} NMR (C_6D_6): 135.0, 127.6, 127.1, 24.7, 24.1, 23.8, 14.0. ^{11}B{^{1}H} NMR (C_6D_6): 11.0. Anal. Calcd: C, 63.64; H, 9.50; N, 4.12. Found: C, 63.39; H, 9.73; N, 4.08.

Synthesis of [(*μ*-R$_3$PN)AlH$_2$]$_2$ [R = *i*-Pr (10), *t*-Bu (11)]. These compounds were prepared in a similar fashion, and thus only one preparation is detailed. To a solution of **1** (2.036 g, 11.620 mmol) in 40 mL of toluene was added 23.22 mL of a 0.5 M solution of AlH_3·NMe_2Et in toluene. Gas evolution was observed upon the addition of the alane complex. The solution was stirred for 16 h, after which the solution was reduced to a white slurry in vacuo, followed by the addition of 20 mL of pentane. The resulting mixture was filtered, and a fine white powder was collected, washed with 5 mL of pentane, and dried in vacuo in 79% yield. **10**. ^{1}H NMR (C_6D_6): 1.98 (d of sept, 6H, $^2J_{P-H}$ = 11 Hz, $^3J_{H-H}$ = 3 Hz), 1.11 (d of d, 36H, $^3J_{H-H}$ = 14 Hz, $^3J_{H-H}$ = 7 Hz). ^{31}P{^{1}H} NMR (C_6D_6): 46.6 (s). ^{13}C{^{1}H} NMR (C_6D_6): 26.9 (d, $^1J_{P-C}$ = 62 Hz), 17.6 (s). ^{27}Al{^{1}H} NMR (C_6D_6): 122.5 (br). Anal. Calcd for $C_{18}H_{46}Al_2N_2P_2$: C, 53.19; H, 11.41; N, 6.89. Found: C, 53.05; H, 11.39; N, 6.49. **11**. Yield: 80%. Some of the white powder was dissolved in minimal amounts of toluene and stored at −33 °C in which X-ray-quality crystals were grown. ^{1}H NMR (C_6D_6): 1.43 (d, 54H, $^3J_{P-H}$ = 13 Hz). ^{31}P{^{1}H} NMR (C_6D_6): 58.0 (s). ^{13}C{^{1}H} NMR (C_6D_6): 42.2 (d, $^1J_{P-C}$ = 62 Hz), 30.9 (s). ^{27}Al{^{1}H} NMR (C_6D_6): 120.4 (br). Anal. Calcd for $C_{24}H_{58}Al_2N_2P_2$: C, 58.75; H, 11.92; N, 5.71. Found: C, 58.21; H, 12.06; N, 5.10.

Synthesis of [(*μ*-*t*-Bu$_3$PN)AlH(O$_3$SCF$_3$)]$_2$ (12). To a solution of **11** (2.00 g, 4.07 mmol) in 20 mL of toluene was added 2.17 g of $Me_3SiO_3SCF_3$. The solution was stirred for 16 h, during which time a white precipitate formed. The precipitate was allowed to settle, and the solvent was decanted off. The white solid was washed with 2 mL of pentane and dried in vacuo. A white fine powder was isolated in 82% yield. ^{1}H NMR (CD_3CN): 1.49 (d, 54H, $^3J_{P-H}$ = 14 Hz). ^{31}P NMR (CD_3CN): 72.2 (s). ^{13}C{^{1}H} NMR (CD_3CN): 29.3 (s), 1.8 (q, J_{F-C} = 21 Hz), 1.7 (q, J_{F-C} = 21 Hz), (d, $^1J_{P-C}$ = Hz), (s). ^{19}F{^{1}H} NMR: −78.9. ^{27}Al{^{1}H} NMR (CD_3CN): 69.9 (br). Anal. Calcd for $C_{26}H_{56}Al_2F_6N_2P_2O_6S_2$: C, 39.69; H, 7.17; N, 3.56. Found: C, 40.01; H, 7.39; N, 3.72.

Synthesis of *t*-Bu$_3$PNBCl$_2$ (14). To a suspension of **13** (150 mg, 0.672 mmol) in 10 mL of ether was added a solution of BCl_3 (225 *μ*L, 1 M solution in heptane, 0.225 mmol). The resulting white suspension was stirred overnight, and then the solvent was evaporated. The product was dissolved in toluene, filtered, and dried in vacuo, resulting in isolation of **14** in 78% yield. ^{1}H NMR (C_6D_6): 1.14 (d, $^3J_{P-H}$ = 14 Hz, 27H). ^{13}C{^{1}H} NMR (C_6D_6): 39.8 (d, $^1J_{P-C}$ = 52 Hz), 28.8 (s). ^{31}P{^{1}H} NMR (C_6D_6): 41.7. ^{11}B{^{1}H} NMR (C_6D_6): 20.3 (br, s). Anal. Calcd for $C_{12}H_{27}BCl_2NP$: C, 48.36; H, 9.13; N, 4.70. Found: C, 48.19; H, 9.01; N, 4.31.

Synthesis of *t*-Bu$_3$PNBMe$_2$ (15). To a solution of **14** (75 mg, 0.252 mmol) in 5 mL of toluene was added MeMgBr (168 *μ*L, 3 M solution in ether, 0.504 mmol). The resulting white suspension was stirred for 1 h and filtered, and the solvent was evaporated, isolating the product as a white powder in 64% yield. ^{1}H NMR (C_6D_6): 1.17 (d, $^3J_{P-H}$ = 13 Hz, 27H), 0.87 (s, 6H). ^{13}C{^{1}H} NMR (C_6D_6): 40.3 (d, $^1J_{P-C}$ = 53 Hz), 29.9 (s), 26.5 (s). ^{31}P{^{1}H} NMR (C_6D_6): 31.1. ^{11}B{^{1}H} NMR (C_6D_6): 45.0 (br s). Anal. Calcd for $C_{14}H_{33}BNP$: C, 65.38; H, 12.93; N, 5.45. Found: C, 64.81; H, 12.02; N, 5.21.

Synthesis of [*t*-Bu$_3$PNBMe]$_2$[(MeB(C$_6$F$_5$)$_3$)]$_2$ (16). To a solution of **15** (20 mg, 0.08 mmol) in 2 mL of CD_2Cl_2 was added $B(C_6F_5)_3$ (40 mg, 0.08 mmol). A white suspension formed instantly. Removal of the solvent resulted in isolation of the product in >95% yield. ^{1}H NMR (C_6D_6): 1.52 (d, $^3J_{P-H}$ = 15 Hz, 27H), 1.18 (s, 3H), 0.46 (br, 3H). ^{13}C{^{1}H} NMR (C_6D_6): 150.0, 148.0, 139.2, 137.3 (br s), 40.9 (d, $^1J_{P-C}$ = 54 Hz), 31.7 (s), 30.3 (s), 27.9 (s). ^{31}P{^{1}H} NMR (C_6D_6): 63.0. ^{11}B{^{1}H} NMR (C_6D_6): 23.0 (br s), −19.1 (s). ^{19}F NMR (CD_2Cl_2): −55.9 (d, $^3J_{F-F}$ = 21 Hz, 6F), −88.1 (m, 3F), −90.7 (t, $^3J_{F-F}$ = 23 Hz). Anal. Calcd for $C_{32}H_{33}B_2F_{15}NP$: C, 49.97; H, 4.32; N, 1.82. Found: C, 49.72; H, 3.90; N, 1.61.

Synthesis of [(*t*-Bu$_3$PN)$_2$B]Cl (17). To a suspension of **5** (100 mg, 0.448 mmol) in toluene (10 mL) was added BCl_3 (0.224 mmol, 224 *μ*L, 1 M in heptane). The resulting white suspension was refluxed overnight, the solvent evaporated, the product dissolved in toluene, and the solution filtered. Compound **17** crystallized in 72% yield. ^{1}H NMR (CD_2Cl_2): 1.46 (d, $^3J_{P-H}$ = 14 Hz, 54H). ^{13}C-{^{1}H} NMR (CD_2Cl_2): 40.7 (d, $^1J_{P-C}$ = 48 Hz), 29.3 (s). ^{31}P{^{1}H} NMR (CD_2Cl_2): 55.7. ^{11}B{^{1}H} NMR (CD_2Cl_2): 11.9 (br). ^{1}H NMR (C_6D_6): 1.35 (d, $^3J_{P-H}$ =13 Hz, 54H). ^{13}C{^{1}H} NMR (C_6D_6): 41.0 (d, $^1J_{P-C}$ = 53 Hz), 30.2 (s). ^{31}P{^{1}H} NMR (C_6D_6): 28.5. ^{11}B{^{1}H} NMR (C_6D_6): −6.1 (br). Anal. Calcd for $C_{24}H_{54}BClN_2P_2$: C, 60.19; H, 11.37; N, 5.85. Found: C, 59.66; H, 11.80; N, 5.47.

Synthesis of (*t*-Bu$_3$PN)$_2$BMe (18). To a suspension of **16** (25 mg, 0. 052 mmol) in 2 mL of toluene was added MeLi (40 *μ*L, 1.4 M solution in ether, 0.056 mmol). The resulting white suspension was stirred over night, filtered and the solvent was evaporated. The product was isolated as a white powder in 69% yield. ^{1}H NMR (C_6D_6): 1.34 (d, $^3J_{P-H}$ = 13 Hz, 54H), 0.9 (s, 3 H). ^{13}C{^{1}H} NMR (C_6D_6) (partial): 41.0 (d, $^1J_{P-C}$ = 53 Hz), 30.5 (s). ^{31}P{^{1}H} NMR (C_6D_6): 20.1 (s). ^{11}B{^{1}H} NMR (C_6D_6): 29.8 (br). Anal. Calcd for $C_{25}H_{57}BN_2P_2$: C, 52.02; H, 9.95; N, 4.85. Found: C, 51.81; H, 9.75; N, 4.96.

Synthesis of [(*t*-Bu$_3$PN)$_2$B][B(C$_6$F$_5$)$_4$] (19) and [(*t*-Bu$_3$PN)$_2$B]-[PF$_6$] (20). These complexes were prepared in a similar manner, and thus only a single representative preparation is described. To a solution of **17** (320 mg, 0.720 mmol) in CH_2Cl_2 (5 mL) was added $[Ph_3C][B(C_6F_5)_4]$ (664 mg, 0.720 mmol). The solution was stirred overnight, the solvent removed in vacuo, and the resulting white powder washed with hexane (2 × 1 mL) and toluene (1 mL). This afforded **19** as a white powder in 65% yield. Uptake of the powder in a minimum amount of toluene and addition of a couple of drops of hexane resulted in isolation of X-ray-quality crystals. **19**. ^{1}H NMR (C_6D_6): 1.46 (d, $^3J_{P-H}$ = 14 Hz, 54H). ^{13}C{^{1}H} NMR (C_6D_6): 150.4−135.2 (br), 40.8 (d, $^1J_{P-C}$ = 48 Hz), 29.3 (s). ^{31}P-{^{1}H} NMR (C_6D_6): 55.0 (s). ^{31}P{^{1}H} NMR (CD_2Cl_2): 55.8 (s).

Table 1. Crystallographic Data

	3	4	8	11	12	21
formula	$C_{27}H_{22}BF_{15}NP$	$C_{30}H_{28}BF_{15}NP$	$C_{12}H_{31}BNP$	$C_{24}H_{58}Al_2N_2P_2$	$C_{26}H_{56}Al_2F_6N_2O_6P_2S_2$	$C_{24}H_{54}B_2F_4N_2P_2$
fw	687.24	729.31	231.16	490.62	786.75	530.25
cryst syst	monoclinic	monoclinic	triclinic	tetragonal	triclinic	tetragonal
space group	$P2(1)/n$	$P2(1)/c$	$P\bar{1}$	$Pa\bar{3}$	$P\bar{1}$	$Pa\bar{3}$
a (Å)	12.331(14)	11.384(18)	8.212(5)	14.486(4)	13.640(8)	14.298(4)
b (Å)	18.87(2)	12.84(2)	8.397(5)		17.599(10)	
c (Å)	12.398(14)	21.46(4)	11.678(6)		19.094(11)	
α (deg)			84.132(12)		112.843(11)	
β (deg)	98.320(16)	91.77(4)	85.683(10)		108.234(12)	
γ (deg)			85.338(10)		90.847(12)	
V (Å^3)	2855(6)	3135(9)	796.7(8)	3039.5(14)	3963(4)	2922.9(16)
Z	4	4	2	4	4	4
d(calc), g cm^{-1}	1.599	1.545	0.964	1.072	1.319	1.205
abs coeff μ, cm^{-1}	0.215	0.200	0.149	0.214	0.325	0.190
data collected	11 220	13 287	3401	12 178	17 049	3111
data $F_o^2 > 3\sigma(F_o^2)$	4055	4451	2262	732	11283	644
variables	406	433	152	56	845	61
R	0.0635	0.0499	0.0551	0.0482	0.0695	0.0588
R_w	0.1378	0.1234	0.1516	0.1423	0.1662	0.1571
GOF	1.082	0.979	1.013	1.058	0.855	1.047

$^{11}B\{^1H\}$ NMR (C_6D_6): 11.1 (br), −20.8 (s). $^{19}F\{^1H\}$ NMR (CD_2Cl_2): −133.4 (s), −164.1 (pst, $^3J_{F-F}$ = 18 Hz), −167.9 (s). Anal. Calcd for $C_{48}H_{54}B_2F_{20}N_2P_2$: C, 51.36; H, 4.84; N, 2.50. Found: C, 51.62; H, 4.94; N, 2.33. **20**. Yield: 66%. ^1H NMR (CD_2Cl_2): 1.47 (d, $^3J_{P-H}$ = 14 Hz, 54H). $^{13}C\{^1H\}$ NMR (CD_2Cl_2): 40.8 (d, $^1J_{P-C}$ = 48 Hz), 29.2 (s). $^{31}P\{^1H\}$ NMR (CD_2Cl_2): 55.9 (s), −144.0 (sept, $^1J_{P-F}$ = 707 Hz). $^{11}B\{^1H\}$ NMR (CD_2Cl_2): −3.9(s). ^{19}F NMR (CD_2Cl_2): 3.8 (d, $^1J_{F-P}$ = 710 Hz). Anal. Calcd for $C_{24}H_{54}BF_6N_2P_3$: C, 48.99; H, 9.24; N, 4.76. Found: C, 48.59; H, 9.34; N, 4.27.

Synthesis of [(μ-*t*-Bu$_3$PN)$_2$BF$_2$]$_2$ (21). To a solution of **17** (50 mg, 0.104 mmol) in 2 mL of CH_2Cl_2 was added Ph_3CBF_4 (34 mg, 0.103 mmol). The resulting red solution was stirred for 2 h, during which time the color disappeared. The solvent was evaporated, and the resulting white powder was washed with hexane. The product is isolated in 86% yield. X-ray-quality crystals were obtained from a saturated CD_2Cl_2 solution of the compound. ^1H NMR (CD_2Cl_2): 1.49 (d, $^3J_{P-H}$ = 14 Hz, 54H). $^{13}C\{^1H\}$ NMR (CD_2Cl_2): 40.7 (d, $^1J_{P-C}$ = 48 Hz), 29.3 (s). $^{31}P\{^1H\}$ NMR (CD_2Cl_2): 55.3 (s). $^{11}B\{^1H\}$ NMR (CD_2Cl_2): 11.8 (br). ^{19}F NMR (CD_2Cl_2): −75.5 (s). Anal. Calcd for $C_{12}H_{27}BF_2NP$: C, 54.36; H, 10.26; N, 5.28. Found: C, 54.50; H, 10.08; N, 4.96.

Molecular Orbital Computations. All density functional theory (DFT) calculations were performed using the *Gaussian 03* suite of programs.[22] The basis set consisted of the B3LYP/6-31g(d) basis set[23−26] on all atoms. The geometries for the computational models were initiated based on the crystallographic results presented herein (Table 1).

X-ray Data Collection and Reduction. Crystals were manipulated and mounted in capillaries in a glovebox, thus maintaining a dry O_2-free environment for each crystal. Diffraction experiments were performed on a Siemens SMART system CCD diffractometer. The data ($4.5° < 2\theta < 45-50.0°$) were collected in a hemisphere of data in 1329 frames with 10 s exposure times. The observed extinctions were consistent with the space groups in each case. A measure of decay was obtained by re-collecting the first 50 frames of each data set. The intensities of the reflections within these frames showed no statistically significant change over the duration of the data collections. The data were processed using the *SAINT* and *SHELXTL* processing packages. An empirical absorption correction based on redundant data was applied to each data set. Subsequent solution and refinement was performed using the *SHELXTL* solution package.

Structure Solution and Refinement. Non-H atomic scattering factors were taken from the literature tabulations.[27] The heavy-atom positions were determined using direct methods, employing the *SHELXTL* direct methods routine. The remaining non-H atoms were located from successive difference Fourier map calculations. The refinements were carried out by using full-matrix least-squares techniques on F^2, minimizing the function $\omega (F_o - F_c)^2$, where the weight ω is defined as $4F_o^2/2\sigma(F_o^2)$ and F_o and F_c are the observed and calculated structure factor amplitudes, respectively. In the final cycles of each refinement, all non-H atoms were assigned anisotropic temperature factors in the absence of disorder or insufficient data. In the latter cases, atoms were treated isotropically. C−H atom positions were calculated and allowed to ride on the C to which they are bonded, assuming a C−H bond length of 0.95 Å. H-atom temperature factors were fixed at 1.10 times the isotropic temperature factor of the C atom to which they are bonded. The H-atom contributions were calculated but not refined. The locations of the largest peaks in the final difference Fourier map calculation as well as the magnitude of the residual electron densities in each case were of no chemical significance. Additional details are provided in the Supporting Information.

(22) Frisch, M. J.; Trucks, G. W.; Schlegel, H. B.; Scuseria, G. E.; Robb, M. A.; Cheeseman, J. R.; Zakrzewski, V. G.; Montgomery, J. A. J.; Stratmann, R. E.; Burant, J. C.; Dapprich, S.; Millam, J. M.; Daniels, A. D. K. K. N.; Strain, M. C.; Farkas, O.; Tomasi, J.; Barone, V.; Cossi, M.; Cammi, R.; Mennucci, B.; Pomelli, C.; Adamo, C.; Clifford, S.; Ochterski, J.; Petersson, G. A.; Ayala, P. Y.; Cui, Q.; Morokuma, K.; Salvador, P.; Dannenberg, J. J.; Malick, D. K.; Rabuck, A. D.; Raghavachari, K.; Foresman, J. B.; Cioslowski, J.; Ortiz, J. V.; Baboul, A. G.; Stefanov, B. B.; Liu, G.; Liashenko, A.; Piskorz, P.; Komaromi, I.; Gomperts, R.; Martin, R. L.; Fox, D. J.; Keith, T.; Al-Laham, M. A.; Peng, C. Y.; Nanayakkara, A.; Challacombe, M.; Gill, P. M. W.; Johnson, B.; Chen, W.; Wong, M. W.; Andres, J. L.; Gonzalez, C.; Head-Gordon, M.; Replogle, E. S.; Pople, J. A. *Gaussian 03*; Gaussian, Inc.: Pittsburgh, PA, 2001.

(23) Ditchfield, R.; Hehre, W. J.; Pople, J. A. *J. Chem. Phys.* **1971**, *54*, 724.

(24) Hariharan, P. C.; Pople, J. A. *Theor. Chim. Acta* **1973**, *28*, 213.

(25) Hariharan, P. C.; Pople, J. A. *Mol. Phys.* **1974**, *27*, 209.

(26) Hehre, W. J.; Ditchfield, R.; Pople, J. A. *J. Chem. Phys.* **1972**, *56*, 2257.

(27) Cromer, D. T.; Waber, J. T. *Int. Tables X-Ray Crystallogr.* **1974**, *4*, 71.

Scheme 1

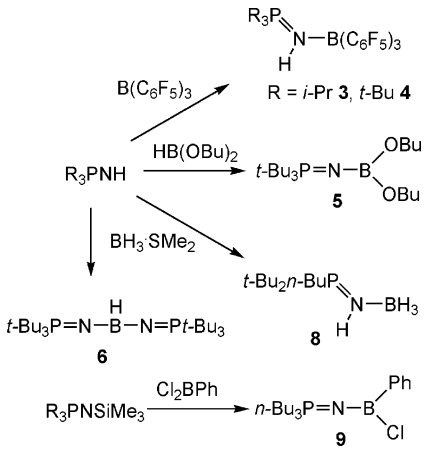

Discussion

We have previously described the formation of the phosphinimine adduct $(Me_3PNSiMe_3)B(C_6F_5)_3$ in which the N−B bond is typical of a Lewis acid−base interaction.[12] In contrast, sterically demanding (trimethylsilyl)phosphinimines react with $B(C_6F_5)_3$, resulting in the abstraction of a methyl group from Si to give species such as $[R_3PNSiMe_2(N(PR_3)SiMe_3][MeB(C_6F_5)_3]$ (R = *i*-Pr, Ph) and $[(\mu\text{-}t\text{-}Bu_3PN)SiMe_2][MeB(C_6F_5)_3]$.[12] In probing of the reactivity of the parent phosphinimines, the corresponding reactions of R_3PNH [R = *i*-Pr (**1**), *t*-Bu (**2**)] with $B(C_6F_5)_3$ were investigated. These reactions proceed under mild conditions and in a facile fashion to form the white crystalline adducts $(R_3PNH)B(C_6F_5)_3$ [R = *i*-Pr (**3**), *t*-Bu (**4**)] in yields of 93 and 95%, respectively (Scheme 1). The ^1H, $^{13}C\{^1H\}$, and ^{19}F NMR spectra of compound **3** are as expected, with a ^1H NMR resonance attributable to the NH proton at 2.97 ppm. The $^{31}P\{^1H\}$ NMR resonance is shifted downfield to 64.0 ppm, consistent with coordination of B to N. The $^{11}B\{^1H\}$ NMR signal is seen at −7.5 ppm, typical of four-coordinate B centers. In a similar sense, compound **4** gives rise to a ^1H NMR resonance at 3.30 ppm from the NH group and $^{31}P\{^1H\}$ and $^{11}B\{^1H\}$ NMR signals at +78.8 and −9.5 ppm, respectively. The formulations of these phosphinimine−borane adducts were unambiguously confirmed via X-ray crystallography (Figures 1 and 2). The B−N distances in **3** and **4** were found to 1.584(8) and 1.614(4) Å, respectively. The longer B−N distance in **4** is attributed to the steric demands of the *tert*-butyl substituents. Notably, the P−N distances of 1.620(5) and 1.649(3) Å and the B−N−P angles of 144.1(4)° and 148.70(17)° in **3** and **4**, respectively, also reflect the influence of the greater steric demands in **4**.

The parent phosphinimine **2** reacts with $HB(OBu)_2$, with evolution of H_2 ultimately affording the fine white powder **5** in 95% yield. This product **5** exhibits a $^{31}P\{^1H\}$ NMR signal at 38.4 ppm as well as a $^{11}B\{^1H\}$ NMR resonance at 17.1 ppm. These data are consistent with the formulation of **5** as $t\text{-}Bu_3PNB(OBu)_2$, in which the B center is three-coordinate (Chart 1). Despite repeated efforts, this could not be confirmed by X-ray crystallography because efforts to obtain suitable crystals were unsuccessful. Nonetheless, this

Figure 1. POV-ray drawing of **3**. Color code: C, black; N, light blue; B, blue; P, orange; F, pink; H, gray. H atoms except for the NH are omitted for clarity. Selected distances (Å) and angles (deg): P−N 1.620(5), N−B 1.584(8), B−N−P 144.1(4).

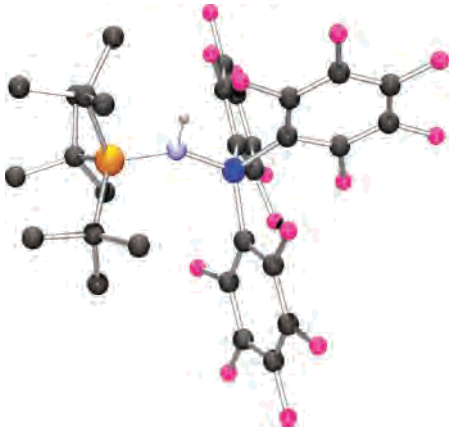

Figure 2. POV-ray drawing of **4**. Color code: C, black; N, light blue; B, blue; P, orange; F, pink; H, gray. H atoms except for the NH are omitted for clarity. Selected distances (Å) and angles (deg): P−N 1.649(3), N−B 1.614(4), B−N−P 148.70(17).

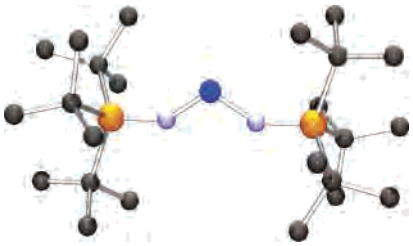

Figure 3. POV-ray drawing of **6**. Color code: C, black; N, light blue; B, blue; P, orange. H atoms are omitted for clarity. Selected distances (Å) and angles (deg): P−N 1.535(7), B−N 1.41(5), N−B−N 117(2), B−N−P 148.2(16).

species is thought to be structurally analogous to the previously reported $t\text{-}Bu_3PNB(O_2C_2Me_4)$.[19]

In a similar protonolysis reaction, 2 equiv of **2** with $BH_3{\cdot}SMe_2$ under reflux afforded the white powder **6** in 75% yield (Scheme 1). Similar to **5**, the $^{31}P\{^1H\}$ NMR resonance of **6** was at 31.2 ppm and the $^{11}B\{^1H\}$ NMR signal at 24.6 ppm; nonetheless, the data did not provide an unambiguous formulation. A single-crystal X-ray diffraction study of **6** confirmed this formulation as $(t\text{-}Bu_3PN)_2BH$ (Figure 3).[20] The structural refinement shows a 6-fold disorder of a B atom about the center of the −3 symmetry. The N−B−N bend is approximately 117(2)°, while the angle at P−N−B

Figure 4. POV-ray drawing of **8**. Color code: C, black; N, light blue; B, blue; P, orange. H atoms except for the BH and NH hydrogens are omitted for clarity. Selected distances (Å) and angles (deg): P−N 1.592(3), N−B 1.580(5), B−N−P 130.6(3).

is 148.2(2)°. The P−N and B−N distances are 1.535(7) and 1.41(5) Å, respectively.

A similar reaction of 1 equiv of the phosphinimine **7** with BH_3·SMe_2 resulted in the formation of X-ray-quality crystals of **8** in 87% yield. The ^{1}H NMR spectrum shows a signal at 0.84 ppm attributable to three BH protons. The dramatic downfield shift of the ^{31}P{^{1}H} NMR resonance to 61.6 ppm and the ^{11}B{^{1}H} NMR chemical shift of −21.0 ppm suggest the formulation of **8** as *n*-Bu(*t*-Bu)$_2$PNH·BH_3 (Scheme 1). This formulation was unambiguously confirmed via a crystallographic study of **8** (Figure 4). Interestingly, the P−N and N−B distances in **8** of 1.592(3) and 1.580(5) Å, respectively, are significantly shorter than those seen in the $B(C_6F_5)_3$ adducts, **3** and **4**. The B−N−P angle in **8** was found to be 130.6(3)°, which is also significantly smaller than those seen in **3** and **4**. These findings are consistent with the weaker Lewis acidity and steric demands of BH_3 versus $B(C_6F_5)_3$. Compound **8** was formed even in the presence of 2 equiv of the phosphinimine **7** and under reflux conditions. This is perhaps surprising because this stands in contrast to the reaction of the phosphinimine **2**. This finding suggests that steric demands encourage H_2 elimination. It is noteworthy that steric demands also have been shown to impact the reactions of phosphinimines R_3PNH with HBpin (pin = $O_2C_2Me_4$). In these cases, sterically demanding phosphinimines prompted H_2 elimination to give $R_3PNBpin$, whereas smaller phosphinimines were reduced to give free phosphine and HN(Bpin)$_2$.[18,19]

An alternative strategy to borane−phosphinimide complexes is exemplified by the reaction of BCl_2Ph with *n*-Bu_3-$PNSiMe_3$. Under a static vacuum for 72 h, this reaction proceeds to evolve $SiMe_3Cl$ and, subsequently, to afford the formation of the white solid **9** in near-quantitative yields (Scheme 1). This formulation was consistent with the ^{1}H and ^{13}C{^{1}H} NMR data as well as the downfield shifts of the ^{31}P{^{1}H} and ^{11}B{^{1}H} NMR resonances to 39.8 and 11.0 ppm, respectively. Efforts to confirm this crystallographically were unsuccessful because of the inability to obtain X-ray-quality crystals despite repeated attempts.

The corresponding reactions of the phosphinimines **1** and **2** with AlH_3·NMe_2Et proceed in a facile fashion with gas evolution, ultimately affording the white solids **10** and **11** in 79 and 80% yield, respectively. While the ^{1}H and ^{13}C-{^{1}H} NMR data for these compounds were consistent with

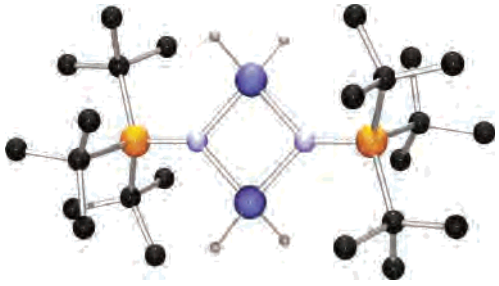

Figure 5. POV-ray drawing of **11**. Color code: C, black; N, light blue; Al, rich blue; F, pink; H, gray; P, orange. H atoms are omitted for clarity. Selected distances (Å) and angles (deg): Al−N 1.887(3), Al′−N 1.905(3), P−N 1.598(4), N−Al−N 89.86(19), P−N−Al 134.65(11).

Scheme 2

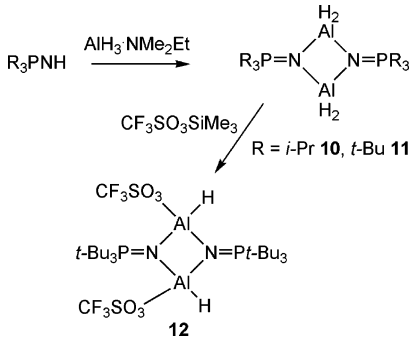

the presence of the R_3P fragment, the observation of ^{31}P-{^{1}H} NMR chemical shifts at 46.6 and 57.8 ppm and ^{27}Al NMR resonances at 122.5 and 120.4 ppm for **10** and **11**, respectively, support coordination of phosphinimide to four-coordinate Al centers. Given that the elemental analysis of these products suggested the empirical formula R_3PNAlH_2, these products were formulated as **10** and **11** (Scheme 2). In the latter case, this formulation was unambiguously confirmed by an X-ray diffraction study (Figure 5). Similar to **6**, the crystal packing of **11** is dominated by the *t*-Bu_3PN ligands, resulting in a disorder of the AlH_2 units. However, in this case, the site occupancy revealed that two Al centers are bridged by the phosphinimide ligands. The Al−N distances were found to range from 1.887(3) to 1.905(3) Å, significantly longer than the B−N distances and yet consistent with typical Al−NPR_3 bridges. The N−Al−N and Al−N−Al′ angles in these four-membered rings were determined to be 89.9(2)° and 90.1(2)°, respectively. These values are similar to those previously reported for the species [(*μ*-*t*-Bu_3PN)$AlMe_2$]$_2$.[13] The corresponding P−N distance in **11** was found to be 1.598(4) Å, while the P−N−Al angle was found to be 134.7(1)°. The parameters are also similar to those reported for [(*μ*-*t*-Bu_3PN)$AlMe_2$]$_2$ although slightly smaller than those seen in [(*μ*-*t*-Bu_3PN)$AlCl_2$]$_2$, consistent with the more electron-deficient Al center in **11** and [(*μ*-*t*-Bu_3PN)$AlMe_2$]$_2$.[13] It is noteworthy that, despite the fact that **6** and **11** are formed in similar fashions, the former species contains only a single B center while the Al analogue is dimeric. This presumably is attributable to the longer Al−N bond distances that accommodate the bridging phosphinimide motif.

Compound **10** reacts with 2 equiv of $Me_3SiO_3SCF_3$ to yield a new species **12**, which gives rise to a new ^{31}P NMR signal

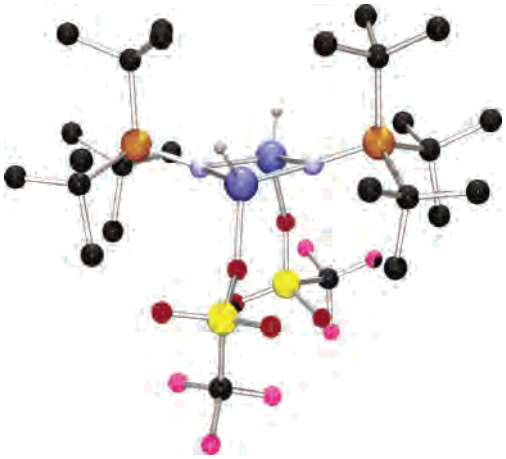

Figure 6. POV-ray drawing of **12** (one molecule from the asymmetric unit is shown). Color code: C, black; N, light blue; Al, rich blue; O, red; S, yellow; F, pink; H, gray; P, orange. H atoms are omitted for clarity. Selected distances (Å) and angles (deg): Al−O 1.828(4), 1.811(4), Al−N 1.875(5), 1.878(5), 1.866(5), 1.889(5), Al−Al′ 2.626(3), P−N 1.612(5), 1.625(5), O−Al−N 107.7(2), 110.3(2), 108.3(2), 110.1(2), N−Al−N 90.9(2), 90.8(2), P−N−Al 135.1(3), 132.9(3).

at 72.2 ppm. This product was isolated in 82% yield (Scheme 2). ^{19}F NMR confirms the presence of the triflate fragments with a resonance at −78.9 ppm. The nature of **12** was confirmed unambiguously via X-ray crystallography as [(μ-*t*-Bu_3PN)AlH(OSO_2CF_3)]$_2$ (Figure 6). Compound **12** is also a dimer in which two phosphinimide ligands bridge two Al centers. However, in addition to one hydride, a triflate group is coordinated through O to Al. The disposition of the triflate groups is pseudo-cis; that is, the two triflate groups are positioned on the same side of the Al_2N_2 core. This orientation presumably is viewed as a steric compromise, yielding lesser triflate−phosphinimide steric conflicts. Because there are two molecules in the asymmetric unit, Al−O distances in **12** were found to range between 1.787(5) and 1.828(4) Å, while the Al−N bond lengths fall in between 1.870(5) and 1.889(5) Å. The O−Al−N angles are approximately tetrahedral, ranging from 107.7(2)° to 110.3(2)°. The Al_2N_2 cores are approximately square, with N−Al−N angles falling in the narrow range of 90.8(2)−91.0(2)°, while the Al−N−Al angles fall between 88.4(2)° and 89.1(2)°. These core metrics result in an average Al···Al′ distance of 2.624(3) Å. The P−N distances in **12** are longer than those in **11**, ranging from 1.607(5) to 1.625(5) Å, while the corresponding P−N−Al angles were found to vary from 132.9(3)° to 135.1(3)°. The observation of longer P−N bonds and shorter Al−N distances in **12** compared to **10** supports the notion of a more electron-deficient Al center in **12**.

An alternative strategy to complexes containing phosphinimide ligands involves the reactions of the lithium salt **13**.[9] Reaction of **13** with BCl_3 proceeds smoothly to give a white solid **14** in 78% yield (Scheme 3). Coordination of phosphinimide to the B center is indicated by the shift of the ^{31}P{^{1}H} NMR signal to 41.7 ppm and the observation of the ^{11}B NMR resonance at 20.3 ppm. This latter point suggests that **14** contains a three-coordinate B center, while elemental analysis was consistent with the formulation of **14** as *t*-Bu_3PNBCl_2. Derivatization of **14** was accomplished

Scheme 3

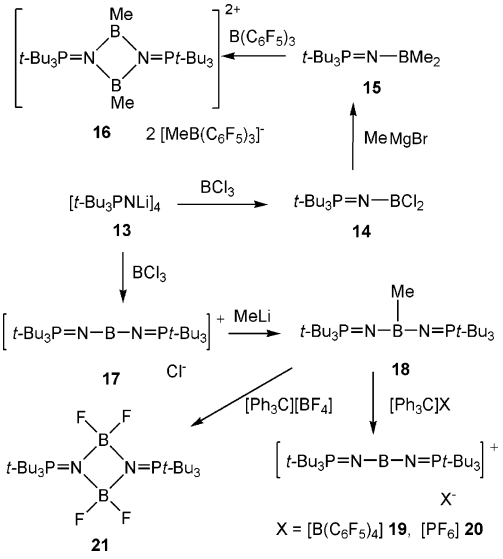

via the subsequent reaction with MeMgBr, affording the species **15** in 64% isolated yield. The ^{1}H and ^{13}C{^{1}H} NMR data were consistent with the formulation of **15** as *t*-Bu_3-$PNBMe_2$ (Scheme 2). The ^{31}P{^{1}H} NMR resonance of **15** shifts upfield to 31.1 ppm. The presence of a three-coordinate B center in **15** is supported by the downfield ^{11}B NMR signal at 45.0 ppm. Subsequent reaction of **15** with $B(C_6F_5)_3$ results in the formation of **16** in >95% yield. The ^{31}P{^{1}H} NMR resonance of **16** shifts dramatically upfield to 63.0 ppm. The ^{1}H NMR spectrum of **16** shows two resonances attributable to B-bound methyl groups at 1.18 and 0.46 ppm, with the corresponding ^{13}C NMR resonances at 30.3 and 27.9 ppm. The ^{11}B NMR spectrum of **16** shows two resonances at 23.0 and −19.1 ppm consistent with the presence of both three- and four-coordinate B centers. These data are consistent with the presence of the anion [$MeB(C_6F_5)_3$] and thus support the formulation of **16** as [(μ-*t*-Bu_3PN)BMe]$_2$[$MeB(C_6F_5)_3$]$_2$ (Scheme 3). It has been previously shown that, in the related aluminum chemistry, only one methyl group is abstracted from [$Me_2Al(\mu$-$NPR_3)$]$_2$ upon reaction with $B(C_6F_5)_3$, affording the dimeric monocation [($Me_2Al(\mu$-$NPR_3)_2AlMe$-($MeB(C_6F_5)_3$)].[13]

Reaction of **13** in a 2:1 ratio with BCl_3 in toluene affords after refluxing for 12 h and subsequent isolation a crystalline solid **17** in 72% yield. Compound **17** in CD_2Cl_2 shows a ^{31}P{^{1}H} NMR resonance at 55.7 ppm, and a broad ^{11}B NMR resonance was observed at 11.9 ppm. While these data together with the ^{1}H and ^{13}C NMR spectra confirmed that **17** was distinct from **14**, the nature of **17** could only be confirmed by X-ray crystallography (Figure 7).[20] This study showed **17** to be [(*t*-$Bu_3PN)_2B$]Cl. As previously communicated, this compound is comprised of the −3 symmetric cation [(*t*-$Bu_3PN)_2B]^+$ in which the crystallographic symmetry imposes linearity on the N−B−N and P−N−B angles. The Cl^- anion sits 7.30 Å from the B center. The B−N distance in **17** is 1.258(5) Å. This is significantly shorter than those seen in $B(NPPh_3)_3$ [1.446(8) Å],[17] [$Fc_2B_2(Br)(\mu$-

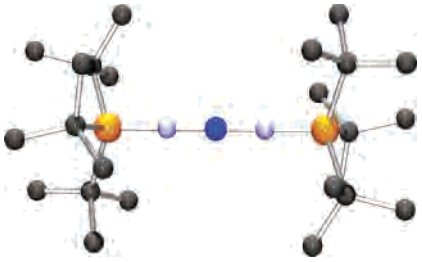

Figure 7. POV-ray drawing of the cation of **17**. Color code: C, black; N, light blue; B, rich blue; P, orange. H atoms are omitted for clarity. Selected distances (Å) and angles (deg): P−N 1.531(5), B−N 1.258(5), N−B−N 180.0(4), B−N−P 180.0(2).

Scheme 4

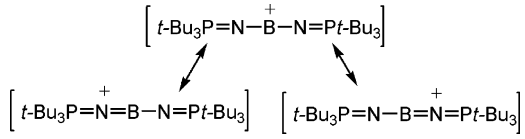

$NPEt_3)_2][Br]$ [Fc = ferrocenyl; 1.44(1) and 1.57(1) Å],[28] $[H_3B_3(NPEt_3)_3Cl_2][Br]$ [1.47(1) Å],[29] $[HBNPEt_3]_3[I]_3$ [1.43(1) Å],[30] $[Bn(Me_3C)N)_2B][AlCl_4]$ [1.33(3) Å], and $[(Me_2N)B(NC_5H_6Me_4)]^+$ [1.30(4) and 1.42(4) Å],[31] consistent with the cationic nature of **17**. The P−N bond length in **17** is 1.531(5) Å, typical of main-group phosphinimide derivatives.

The formation of **17** exclusively occurs even in the presence of excess **13**. Smaller phosphinimides have been shown to result in trisubstitution, as is the case in the formation of $B(NPPh_3)_3$.[17] The steric demands present in **17** result in the spontaneous dissociation of halide from the B center. Although bulky amidoborinium ions were reviewed by Kölle and Nöth[31] two decades ago, the linear geometry of the PNBNP atoms in the cation of **17** is, to our knowledge, the first example of a borinium ion formed spontaneously instead of via halide abstraction with a Lewis acid. The stability of this linear cationic arrangement of five atoms is undoubtedly related to resonance forms that distribute the cationic charge onto the N atoms (Scheme 4).

Compound **17** reacts with MeLi to form a species formulation $(t\text{-}Bu_3PN)_2BMe$ (**18**) in 69% yield (Scheme 3). This species, as well as **6**, reacts with $[Ph_3C][B(C_6F_5)_4]$ to abstract methyl or hydride, affording the borinium salt **19** (Scheme 3). This species was also characterized crystallographically.[20] The geometries of the cations of **17** and **19** are very similar, although in the latter case, lesser crystallographic symmetry is imposed, and thus, while a linear geometry at B is required, the geometry at N distorts slightly with a P−N−B angle of 162.1(3)°. The cation and anion in **19** are well-separated. The B−B distance is 10.43 Å.

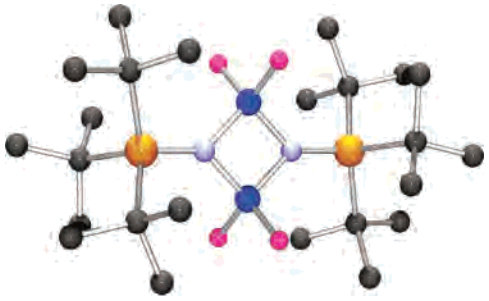

Figure 8. POV-ray drawing of **21**. Color code: C, black; N, light blue; B, blue; F, pink; P, orange. H atoms are omitted for clarity. Selected distances (Å) and angles (deg): P(1)−N(1) 1.597(5), N(1)−B(1) 1.544(16), B(1)−N(1)−P(1) 136.9(5), B(1)−N(1)−P(1) 137.3(6), N(1)−B(1)−N(1) 94.2(8), F(1)−B(1)−F(1) 104.7(16).

In a similar fashion, abstraction of methyl or hydride from **18** or **6** with $[Ph_3C][PF_6]$ afforded the analogous salt **20** (Scheme 3). In contrast, while the analogous reaction of **18** or **6** with $[Ph_3C][BF_4]$ also affords Ph_3CMe or Ph_3CH, respectively, the new product **21** was isolated in these cases. The $^{11}B\{^1H\}$ NMR spectrum exhibited a single broad resonance at 11.8 ppm, and the ^{19}F NMR spectrum showed a resonance at −75.5 ppm, inconsistent with the presence of a $[BF_4]^-$ anion. A crystallographic analysis of **21** revealed that **21** is correctly formulated as $[t\text{-}Bu_3PNBF_2]_2$ (Figure 8 and Scheme 3). Thus, the phosphinimide ligand bridges two BF_2 units. Crystallographic −3 symmetry is imposed, and thus disorder of BF_2 fragments is evident. As a result of this disorder, detailed comments on the metric parameters are inappropriate; however, the B−N bonds in **21** were found to be 1.544(16) Å, which is slightly elongated in comparison to **17** and **19**. The formation of **21** presumably proceeds through a transient formation of the salt $[(t\text{-}Bu_3PN)_2B][BF_4]$, which rapidly undergoes fluoride abstraction and ligand redistribution to form **21**.

The NMR data for the salts **17** and **19** show a marked solvent dependence. The ^{31}P NMR resonance for **17** shifts from 55.7 ppm in CD_2Cl_2 to 28.5 ppm in C_6D_6, whereas the analogous signals for **19** are observed at 55.8 and 55.0 ppm, respectively. The addition of $AlCl_3$ to a benzene solution of **17** sequesters the chloride ion, forming $[AlCl_4]^-$, and the ^{31}P NMR resonance shifts from 28.5 to 55.8 ppm. These data infer that **17** forms a tight ion pair in nonpolar solvents, while in polar solvents, salvation of the ions results in ion-pair separation. These results also suggest that the energy difference between a tight ion pair and the corresponding salt of **17** is small. This view is further supported by the observation that crystals of **17** in which ion-pair separation is confirmed crystallographically were grown from toluene. This suggests that, despite the ion pairing in solution, crystal-packing forces favor the salt. These views are also supported by theoretical predictions of the ^{31}P NMR chemical shifts, as previously communicated.[20]

DFT calculations were performed for the models $[(Me_3PN)_2M]^+$ (M = B, Al) using the B3LYP/6-31g(d) basis set. These models were constructed based on the crystallographic data described herein for **14**. Geometry optimizations and molecular orbital calculations were performed. In both cases, the highest occupied molecular orbital (HOMO; Figure 9a,c)

(28) Mohlen, M.; Neumuller, B.; Pebler, J.; Dehnicke, K. *Z. Anorg. Allg. Chem.* **2001**, *627*, 1508.
(29) Mohlen, M.; Neumuller, B.; Dashti-Mommertz, A.; Muller, C.; Massa, W.; Dehnicke, K. *Z. Anorg. Allg. Chem.* **1999**, *625*, 1631.
(30) Mohlen, M.; Neumuller, B.; Harms, K.; Krautscheid, H.; Fenske, D.; Diedenhofen, M.; Frenking, G.; Dehnicke, K. *Z. Anorg. Allg. Chem.* **1998**, *624*, 1105.
(31) Kölle, P.; Nöth, H. *Chem. Rev.* **1985**, *85*, 399.

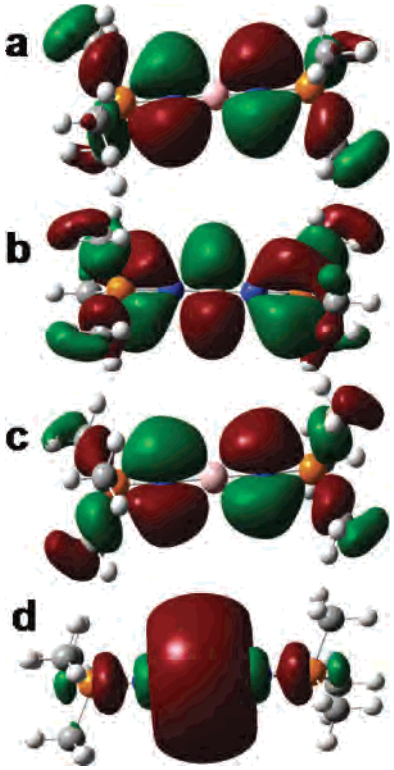

Figure 9. Gaussview depictions of molecular orbitals for the model compounds $[(Me_3PN)_2M]^+$ (M = B, Al). M = B: (a) HOMO; (b) LUMO. M = Al: (c) HOMO; (d) LUMO.

is comprised primarily of the interaction of the N-based p orbital with the P-based d orbital. In the case of the B species, the lowest unoccupied molecular orbital (LUMO; Figure 9b) is comprised of a B-based p orbital mixed with an N−P π orbital. This is consistent with the delocalization of the formal positive charge over the entire P−N−B−N−P chain. In contrast, the LUMO for the hypothetical Al model is based primarily on an Al-based d orbital (Figure 9d). This localization of the positive charge on Al in this model is consistent with the observed propensity of aluminum phosphinimides for dimerization as well as the inability to experimentally synthesize a direct Al analogue of **14**.

Summary

The chemistry described herein presents several strategies for the formation of boron and aluminum phosphinimine and phosphinimide complexes. In general, sterically demanding phosphinimide ligands result in the formation of monomeric B species, whereas in the related Al compounds, the phosphinimide ligands bridge Al centers, resulting in dimeric products. The chemistry of main-group phosphinimides continues to be a subject of study in our laboratories.

Acknowledgment. Financial support from NSERC of Canada is gratefully acknowledged.

Supporting Information Available: Crystallographic data in CIF format. This material is available free of charge via the Internet at http://pubs.acs.org.

IC0700351